Effective Hamiltonian in the Problem of a "Central Spin" Coupled to a Spin Environment

EFFECTIVE HAMILTONIAN IN THE PROBLEM OF A "CENTRAL SPIN" COUPLED TO A SPIN ENVIRONMENT

I. S. Tupitsyn[1], N. V. Prokof'ev[1,2], P. C. E. Stamp[2]
[1] *Russian Science Center "Kurchatov Institute", Moscow 123182, Russia*

[2] *Physics Department, University of British Columbia, 6224 Agricultural Rd., Vancouver B.C., Canada V6T 1Z1*

We consider here the problem of a "giant spin", with spin quantum number $S \gg 1$, interacting with a set of microscopic spins. Interactions between the microscopic spins are ignored. This model describes the low-energy properties of magnetic grains or magnetic macromolecules (ferromagnetically or antiferromagnetically ordered) interacting with a surrounding spin environment, such as nuclear spins.

Our aim is to give a general method for truncating the model to another one, valid at low energies, in which a two-level system interacts with the environmental spins, and higher energy terms are absorbed into a new set of couplings. This is done using an instanton technique.

We then study the accuracy of this technique, by comparing the results for the low energy effective Hamiltonian, with results derived for the original giant spin , coupled to a macroscopic spin, using exact diagonalisation techniques. We find that the low energy central spin effective Hamiltonian gives very accurate results (with increasing accuracy for large S), provided the typical coupling energies between the giant spin and the microscopic spins are not too large, and provided temperature and external field are sufficiently low. The essential limitation to the applicability of the low-energy effective Hamiltonian is just the semiclassical WKB approximation itself, which inevitably fails for very small S.

Our results thus justify previous use of this effective Hamiltonian in calculations of the effects of nuclear spins on the dynamics of nanomagnetic systems.

I. INTRODUCTION

In this paper we examine a model which was originally introduced to deal with the effects of environmental spins on the coherent tunneling of magnetic grain magnetisation [1–3]. It consists of a central "giant spin" [4–6], having spin quantum number $S \gg 1$, coupled to a set $\{\vec{\sigma}_k\}$ of "microscopic spins"; the microscopic spins are only very weakly coupled to each other. The model is then completely described by a Hamiltonian $H_o(\vec{S})$ for the central spin, a Hamiltonian $H_{env}(\{\vec{\sigma}_k\})$ for the microscopic spins, and a coupling $H_{int}(\vec{S}, \{\vec{\sigma}_k\})$ between the two:

$$H(\vec{S}, \vec{\sigma}_k) = H_o(\vec{S}) + \frac{1}{2S}\sum_{k=1}^{N} \omega_k \vec{S} \cdot \vec{\sigma}_k + V_{dip}(\{\vec{\sigma}_k, \vec{\sigma}_{k'}\}) \; , \tag{1.1}$$

in which we specialise immediately to the form relevant to most of this paper, in which the interaction between the central spin and the environment has a hyperfine form, and the dynamics of the environmental spins (considered now to be nuclear spins), comes from their mutual dipolar or indirect Suhl-Nakamura interactions. In most practical applications of this "central spin model", the environmental nuclear spins will be either inside the object carrying the giant spin, or near it, in some substrate, or solvent, or surrounding matrix. The central spin may be a magnetic grain [5] or a magnetic macromolecule such as ferritin [7] or, on a smaller scale [8], Mn_{12}-ac. Similar models were also introduced some time ago to describe the large superparamagnetic "spin clusters" which are believed to exist in many disordered magnets at low temperature, such as $Si:P$ near the metal-insulator transition [9], or "giant magnetic polarons" [10]. Similar spin clusters exist in "quantum spin glasses" [11]. In these models the giant spin is somewhat less uniquely defined (indeed its size depends on temperature). Finally, a similar central spin model was considered a long time ago by Gaudin, who wrote down a set of Bethe ansatz equations for it [12].

We should also note that models like (1.1) can be of interest even for non-magnetic systems (although the coupling term will not then be a hyperfine one). This is because most large quantum objects will have (at least) a coupling to their own nuclei, and perhaps to other quasi-free spin degrees of freedom like paramagnetic impurities. Thus in the oft-cited example of the superconducting SQUID ring [13], there is an electromagnetic coupling of the tunneling flux coordinate (and the associated ring supercurrent) to all of the nuclear spins within a penetration depth of the surface (either in the junction or in the ring), as well as to any paramagnetic impurity spins that happen to be present [14]. The nuclear spins can then not only change the energetics of the relevant collective coordinate, but also dephase it, in a kind of "inverse Stern-Gerlach effect", where nuclear spins play the role of measuring devices [14,15]. It then becomes important to determine how the coupling to the background spins will affect the quantum dynamics of the central system. This depends of course on the system; for example, in the case of SQUID's, it is fairly easy to show that the effect of the environmental nuclear and paramagnetic spins on flux tunneling is usually negligible, but that the effect on "Macroscopic Quantum Coherence" may not be. On the other hand, the strength of the hyperfine coupling, between the order parameter of many nanomagnetic systems and their nuclear spins, is such that the nuclear environment can seriously disrupt the quantum dynamics of the nanomagnet at low T.

The purpose of the present paper is not to analyze the effects of the environmental spin bath on the dynamics of nanomagnet - we have done this in a number of other papers. Instead we wish to investigate the validity of the effective Hamiltonian we have previously employed. This Hamiltonian results from a truncation to a lower-dimensional Hilbert space in which the giant spin dynamics are reduced to that of a two-level system (still coupled to N environmental spins). This truncation is analogous to the truncation of a quantum system like a SQUID, coupled to delocalized electrons, to the "spin-boson" model at low T. In the present case of the central spin, the truncated central spin effective Hamiltonian takes the form

$$H_{eff} = \left\{ 2\Delta_o \hat{\tau}_- \cos\left[\pi S + \sum_k \alpha_k \vec{n} \cdot \hat{\vec{\sigma}}_k - \beta_o \vec{n} \cdot \vec{H}_o \right] + H.c. \right\} + \frac{\hat{\tau}_z}{2} \sum_{k=1}^{N} \omega_k^{\parallel} \vec{l}_k \cdot \hat{\vec{\sigma}}_k + \frac{1}{2} \sum_{k=1}^{N} \omega_k^{\perp} \vec{m}_k \cdot \hat{\vec{\sigma}}_k + \sum_{k=1}^{N} \sum_{k'=1}^{N} V_{kk'}^{\alpha\beta} \hat{\sigma}_k^{\alpha} \hat{\sigma}_{k'}^{\beta} \quad . \tag{1.2}$$

In this Hamiltonian the two-level dynamics of S will be described by the Pauli vector matrix $\hat{\vec{\tau}}$, and we have assumed that $H_o(\vec{S})$ in (1.1) contains an external field $\vec{H}_o$. This is the same form as we have used in previous investigations [3,16]. Here Δ_o is a tunneling matrix element, $\vec{n}$, $\vec{l}_k$, and $\vec{m}_k$ are unit vectors, with $\vec{l}_k$ and $\vec{m}_k$ mutually perpendicular; α_k and β_o are dimensionless parameters, and $\omega_k^{\parallel}$ and $\omega_k^{\perp}$ are "longitudinal" and "transverse" diagonal coupling energies [16].

In the present paper we will show how one goes from (1.1) to (1.2), in an instanton calculation; and we will discuss how accurately (1.2) represents the dynamics of (1.1), by carrying out exact diagonalization studies of (1.1), and comparing them with the predictions of (1.2). To do this we will pick a special (but actually quite generic) form for $H_o(\vec{S})$, viz., a biaxial (easy axis/easy plane) form

$$H_o(\vec{S}) = \frac{1}{S}\left[-K_{\parallel} S_z^2 + K_{\perp} S_y^2 \right] , \tag{1.3}$$

and calculate the parameters in (1.2) deriving from (1.3), in an instanton expansion. We should note here that some similar exact diagonalisation studies of this model were recently carried out by Abarenkova & Angles d'Auriac [17], who also compared their exact diagonalisation results with a somewhat simplified version of (1.2) in certain limits. In the present work we have a rather different aim; we wish to show that the structure of the exact diagonalisation results can be put in a form very close to that in (1.2), and then we can check numerically whether the coefficients in (1.2) agree with those we calculate using an instanton procedure, over a very wide paramenter range. Thus we are not just trying to test the truncated model numerically; we are also trying to test its *form*, and to see if anything is missing from it.

We find that, as assumed in previous work, 1.2) gives a very good description of the low-energy dynamics of (1.1), both as regards the mathematical form and the numerical values calculated for the coefficients in an instanton expansion, *provided* that

(i) The semiclassical approximation for the "bare" giant spin Hamiltonian $H_o(\vec{S})$ is a good one;

(ii) The parameter $E_o = \omega_o N^{1/2}$, characterizing the spread in energies caused by the hyperfine coupling, and the thermal energy $k_B T$, satisfy the inequality $E_o, k_B T \ll \Omega_o$, where Ω_o is the "bounce frequency" associated with semiclassical tunneling, which characterizes roughly the energy gap between the lowest doublet of states of $H_o(\vec{S})$,

and the higher excited states. Thus the result (1.2) can start to fail if either the mean hyperfine coupling ω_o, or the number N of nuclear spins, becomes too large.

(iii) The "bias" energy $\xi_H = \gamma_e(\vec{S}_1 - \vec{S}_2) \cdot \vec{H}_o$, where $\vec{S}_1$ and $\vec{S}_2$ are the two semiclassical minima of $H_o(\vec{S})$, must also satisfy $\xi_H \ll \Omega_o$.

Conditions (ii) and (iii) simply prevent the two lowest levels of $H_o(\vec{S})$ from significantly mixing with higher levels, once the nuclear spins or magnetic field are coupled in.

Although these results are derived for the particular example (1.3), we believe that the instanton method we use can be applied to most reasonable forms of $H(\vec{S}, \{\vec{\sigma}\})$ like (1.1), to give a truncated form like (1.2), provided the same "low-energy" restrictions (i)-(iii) are satisfied; all that will change will be the values of the parameters in (1.2) (for the case (1.1), the values of the parameters appearing in (1.2) are given in Sec. III below).

In what follows we begin (in section II) by describing the central spin model, and giving some discussion of the relevant physical coupling energies in it. In section III we show how an initial microscopic Hamiltonian, describing the giant central spin and its microscopic environmental satellites, can be truncated to a low-energy effective Hamiltonian description. In section IV we proceed to the discussion of the results of the exact diagonalization studies and, finally, in section V, we summarize our results.

II. THE MODEL, AND SOME SIMPLE EXAMPLES

In this section we briefly describe the physical origin of the central spin model for nanomagnetic systems, and the Hamiltonian of eqtn. (1.1), and also remark on what is left out of it. Since the variety of physical examples is rather large, as is the range of possible coupling energies, we also mention some reference examples.

Let us consider first the central spin itself, whose dynamics is described in eqtn. (1.1) by $H_o(\vec{S})$. A typical central spin is made up of a very large number of microscopic spins, whose motion is assumed to be locked together by nearest-neighbour exchange, or "Hund's rule", couplings (or, in the case of superparamagnetic spin complexes, by indirect spin-spin couplings such as the RKKY interaction). These couplings can be very large, as much as $0.1 - 1\,eV$; this is much larger than other individual spin energy scales such as those coming from anisotropy, so that in principle one can have large monodomain magnetic particles, with many spins (up to perhaps 10^8, depending on the particular systems) lined up to form a "giant spin" [4,5,15]. Another more subtle example is the antiferromagnetic grain, in which nearest neighbours are anti-parallel, and one obtains a "giant Néel vector" [18,19]. The superparamagnetic spin complexes are more delicate still, and typically arise at low temperatures when paramagnetic electronic spins in a disordered magnet "lock together" via indirect exchange, RKKY interactions, etc [9].

The first step in analysing such a system is to treat the entire spin complex as a rigid quantum rotator $\vec{S}$, with dynamics governed by an anisotropy field in the particle/grain; i.e., write a central spin "bare Hamiltonian" $H_o(\vec{S})$, with $\mid \vec{S} \mid = S$ a constant. The next step to take, if the temperature is low, is to try truncating a Hamiltonian like (1.3) to a 2-level system, involving only the lowest 2 levels. This has been done by various authors; in fact the papers of van Hemmen and Suto [4] analyzed a much more general class of bare central spin Hamiltonians than (1.3).

The giant spin model omits the higher excited states of the particle, involving spin flips of spins inside the grain (internal magnons); the neglect of these is usually justified by appeal to the large value $\mid J \mid$ of spin exchange [5,15], in models like equation (1.3). Incorporation of such processes implies relaxation of the constraint $\mid \vec{S} \mid$=constant. In most circumstances this will hardly be a serious omission; the lowest "internal magnon" excitations do not even reach the top of the "ginat spin" multiplet of $(2s+1)$ levels until the grain or molecule reaches a radius $L \sim (Ra)^{1/2}$, for an AFM grain (R is the domain wall length, roughly equal to the maximum size of a monodomain magnet; and a is the typical interspin spacing in the magnet); or $L \sim (R^2 a^3)^{1/5}$ for a FM grain. Even when we do get mixing of internal magnon modes and giant spin levels at these energies (i.e., energies $\sim 2SK$, where K is a typical anisotropy term), this will hardly affect either the energetics or dynamics at energy scales $\Omega_o \sim K$ or below. Another omission is that of surface excitations of the system - in any real nanomagnetic grain, there can be low-energy magnetic excitations involving "loose spins", i.e., spins which, because of imperfect preparation or the inevitable defects, dislocations, etc., have a coupling energy $\ll J$ to their neighbours. These couplings are hard to quantify, but it is rather unlikely that they will be as small as the single-ion anisotropy energies in (1.3). We will also ignore the possibility that surface spins might have anisotropy energies differing from those inside the grain.

Finally, in this paper we will ignore all couplings to external bosonic baths such as electrons, phonon, or photons. Electron effects on nanomagnets were recently discussed by us [16] (as well as by Fukuyama and Tatara for domain walls [20]). Phonon effects have been discussed by many authors [21,22]. Photon effects were shown to be negligible

some time ago [23]. Experimental predictions for the behavior of nanomagnets coupled simultaneously to oscillator and spin bath were given in Ref. [16]; the work was also recently applied to the Mn_{12}-acetate system [24].

We now turn to the problem of main interest here, i.e., the coupling of $\vec{S}$ to other spin degrees of freedom - as already noted, we are primarily interested in nuclear spins, both inside and outside the grain. A nucleus with a finite spin I, and spin moment $-\gamma_N \hbar I$, interacts both locally with the electron clouds at the same ionic site, via the contact hyperfine interaction, and also non-locally with other ions via the dipolar field. There may also be other residual interactions such as transfer hyperfine interaction (as for, e.g., F^{19} in MnF_2 or CoF_2), or quadrupolar coupling if $I > 1/2$. Finally, one may have interactions between the different nuclear spins, via, e.g., spin waves (the Suhl-Nakamura interaction), or dipolar couplings - these are very weak (Suhl-Nakamura interactions are $\sim 10^{-6}\,K$, and nuclear dipole-dipole interactions $\sim 10^{-7}\,K$) but, it turns out, can play a role in the dynamics of $\vec{S}$.

The most important interactions are the contact hyperfine interaction $-\gamma_N \hbar \vec{I} \cdot \mathcal{A} \cdot \vec{S}_o$ to the electronic spin on the same ionic site, and the dipolar interaction between the nuclei and electrons. The strength of these interactions is measured directly in NMR experiments; the hyperfine couplings range from $1 - 3\,MHz$ (i.e., $5 - 15 \times 10^{-5} K$) for protons in H^1, up to values greater than $5000\,MHz$ ($0.25\,K$) for some rare-earth magnetic nuclei (e.g., Tb^{159}, Dy^{163}); these latter correspond to local fields acting on the nuclei as high as $500\,Tesla$, and come overwhelmingly from the contact interaction. Thus when a central spin rotates, with all internal electronic spins rotating in unison, the contact interaction tries to force the nuclei on the magnetic sites to follow. If the contact hyperfine interaction strength is ω_o, then it is clear that the ratio ω_o/Ω_o, with Ω_o^{-1} the timescale of central spin rotation, is going to be crucial to the nuclear spin dynamics. The parameter Ω_o for the ferromagnetic grain is defined by the anisotropy energy $\Omega \sim K$, while for the antiferromagnetic grain it is much higher, typically $\Omega \sim 2\sqrt{KJ}$ [18,19]. If the electronic spin frequencies $\Omega_o \gg \omega_o$, then the nuclear spins will experience a "sudden" perturbation, and few of them will follow the central spin; conversely, if $\omega_o \gg \Omega_o$, the nuclear spins will follow adiabatically. In fact, the ratio ω_o/Ω_o is usually somewhere between $0.001 - 0.1$. On the other hand for nuclei in non-magnetic ions, ω_o/Ω_o may be much smaller, and will of course depend strongly on the host (in a magnetic host, transfer hyperfine interactions $-\gamma_N \hbar \vec{I} \cdot \mathcal{A}_{0j} \cdot \vec{S}_j$ from nearby magnetic moments $\vec{S}_j$, can greatly increase ω_o; for example, ω_o for F^{19} in MnF_2 is $160\,MHz$).

A large central spin will also interact with nuclear spins in the surrounding medium (a substrate or solvent) via the dipolar interaction generated by the central spin dipolar field. This interaction may not be negligible; for a central spin with $S = 10^4$, the dipolar coupling to a nucleus at a distance of $100\mathring{A}$ is already $\sim 1\,MHz$, rising to $30\,MHz$ at a distance of $30\mathring{A}$; and there is clearly a very large number of nuclear spins within $100\mathring{A}$ of the central spin! We should also note, that the same considerations may be also applied to quite distant paramagnetic impurities. For $S = 10^4$ they couple to the giant spin in the MHz range up to distances $1000\mathring{A}$.

The approach we shall take is to include first the overwhelmingly dominant hyperfine interaction in the coupling between S and each nuclear spin. Since the individual electronic moments are locked together this leads directly to the second term in (1.1). We will drop the internuclear couplings; these are so weak that their effects can be handled in a very simple way once the main "central spin" problem has been solved, as a weak after-effect [16]. In fact it is trivial to show that the effects of the internuclear dipolar coupling can be entirely handled, in this effective Hamiltonian approach, by adding back the dipolar coupling to the low-energy effective Hamiltonian in exactly the same form as it appears in the high-energy Hamiltonian- this is what we have done in writing equations (1.1) and (1.2). Thus, we shall use, as our starting point for analysis, the model in Eq. (1.1), without the internuclear dipolar interaction.

III. THE EFFECTIVE HAMILTONIAN

The task of this section is to truncate the "giant spin" description, and find a new effective Hamiltonian which operates only at low energies. In fact we reduce the $(2S+1)$-dimensional Hilbert space of the giant spin itself down to two lowest levels - the giant spin is now described by a Pauli vector matrix $\vec{\tau}$. This two-level system interacts with a "spin-bath", described by Pauli matrices $\{\vec{\hat{\sigma}}_k\}$, with $k = 1, 2, 3, \ldots N$. The new effective Hamiltonian thus operates in a reduced Hilbert space, of complex dimension 2^{N+1}. We may use this Hamiltonian H_{eff} *provided* higher energy degrees of freedom are not excited. This means in practice that H_{eff} is restricted to energy scales $\ll \Omega_o$, the characteristic frequency of zero point fluctuations of $\vec{S}$. The higher levels do of course affect H_{eff}; in the usual way, their effects are incorporated into renormalised "coupling constants" in H_{eff}.

In what follows we first explain how the truncation procedure is done for this kind of problem; then we derive H_{eff}, starting from the giant spin model.

A. Free Giant Spin

The technique we use is the standard one of separating the "slow" and "fast" degrees of freedom in the problem; for our giant spin the difference between the two is illustrated in Fig. 1. The truncated Hamiltonian should only include slow variables, the fast ones having been eliminated in favour of a new set of couplings between the slow ones.

Let us first briefly recall how the truncation is done in the *absence* of the environmental spins and magnetic field - this makes the method clear, and also gives us some results we will need later. Since $S \gg 1$, one uses semiclassical methods - the task is to start from a free giant spin Hamiltonian $H_o(\vec{S})$ like (1.3), and derive a reduced Hamiltonian $H^o_{eff}(\vec{\tau})$, operating in the space of the lowest two levels of $H_o(\vec{S})$. We shall choose a basis in this truncated space such that the eigenstates of $\hat{\tau}_z$ correspond to the 2 semiclassical minimum states of $H_o(\vec{S})$, defined by coherent state vectors $|\vec{n}_1\rangle$ and $|\vec{n}_2\rangle$, such that $\langle\vec{n}_1|\vec{S}|\vec{n}_1\rangle = S\vec{n}_1$ and $\langle\vec{n}_2|\vec{S}|\vec{n}_2\rangle = S\vec{n}_2$; the eigenstates of $H^o_{eff}(\vec{\tau})$ are then linear combinations of $|\vec{n}_1\rangle$ and $|\vec{n}_2\rangle$, which we can determine once we have found the four matrix elements $\langle\vec{n}_\alpha|H^o_{eff}|\vec{n}_\beta\rangle$ with $\alpha, \beta = 1, 2$.

Formally one can do this as follows, for the free spin. Consider the path integral expression for the transition amplitude $\Gamma^o_{\alpha\beta}(t)$, during the time t; this is given by [5,15]:

$$\Gamma^o_{\alpha\beta}(t) = \langle\vec{n}_\alpha|e^{-iH_o(\vec{S})t}|\vec{n}_\beta\rangle = \int_{\vec{n}(\tau=0)=\vec{n}_\beta}^{\vec{n}(\tau=t)=\vec{n}_\alpha} \mathcal{D}\vec{n}(\tau) \exp\left\{-\int_0^t d\tau \mathcal{L}_o(\tau)\right\} , \tag{3.1}$$

where the free spin Euclidean Lagrangian is

$$\mathcal{L}_o = -iS\dot{\theta}\varphi\sin\theta + H_o(\vec{n}) . \tag{3.2}$$

Here θ and φ are the usual polar and azimuthal angles for the unit vector $\vec{n}(\tau)$.

Now in the semiclassical approximation there are two fundamental time scales in the paths $\vec{n}(\tau)$ in (3.1); these are Ω_o^{-1}, the time required for the instanton traversal to be made between states, and Δ_o^{-1}, the typical time elapsing between instantons. By definition, an effective Hamiltonian is supposed to reproduce the slow dynamics of the system in the truncated Hilbert space of the two lowest levels, i.e., for long time scales an evolution operator is approximated as

$$\Gamma^o_{\alpha\beta}(t) \approx \left(e^{-iH_{eff}t}\right)_{\alpha\beta} . \tag{3.3}$$

Since Δ_o is exponentially smaller than Ω_o, and nondiagonal elements are $H_{eff} \sim \Delta_o$, we can write

$$\begin{aligned}\Gamma^o_{\alpha\beta}(t) &= \langle\vec{n}_\alpha|e^{-iH_{eff}t}|\vec{n}_\beta\rangle \\ &\approx \delta_{\alpha\beta} - it\langle\vec{n}_\alpha|H^o_{eff}|\vec{n}_\beta\rangle ; \quad (\Omega_o^{-1} \ll t \ll \Delta_o^{-1}) ;\end{aligned} \tag{3.4}$$

Then we immediately find the matrix elements of $H^o_{eff}(\vec{\tau})$ for $\alpha \neq \beta$ as

$$\left(H^o_{eff}(\vec{\tau})\right)_{\alpha\beta} = \frac{i}{t}\Gamma^o_{\alpha\beta}(t) ; \quad (\Omega_o^{-1} \ll t \ll \Delta_o^{-1}) . \tag{3.5}$$

As a concrete example, consider the easy-axis/easy-plane Hamiltonian (1.3), where

$$H_o(\vec{n}) = SK_\parallel\left[\sin^2\theta + \frac{K_\perp}{K_\parallel}\sin^2\theta\sin^2\varphi\right] , \tag{3.6}$$

The two lowest states are $\vec{n}_1 = \hat{\vec{z}}$ and $\vec{n}_2 = -\hat{\vec{z}}$; henceforth we write these states as $|\Uparrow\rangle$ and $|\Downarrow\rangle$. In the usual case where $K_\perp/K_\parallel \gg 1$ (so that the tunneling amplitude is appreciable) one has only small oscillations of φ about the semiclassical trajectories $\varphi = 0$ or π, and by eliminating φ one has

$$\mathcal{L}_o(\theta) = \frac{S}{4K_\perp}\dot{\theta}^2 + SK_\parallel\sin^2\theta , \tag{3.7}$$

giving a classical equation of motion $\dot{\theta} = \Omega_o\sin\theta$, and instanton solution [5,15], going from $|\Uparrow\rangle$ to $|\Downarrow\rangle$

$$\sin\theta(\tau) = 1/\cosh(\Omega_o\tau) \tag{3.8}$$

(centered at $\tau = 0$); in this system

$$\Omega_o = 2(K_\parallel K_\perp)^{1/2} \ . \tag{3.9}$$

The frequency Ω_o then sets the ultraviolet cut-off for the Hilbert space of $H^o_{eff}(\vec{\tau})$, and one finds, by substituting the semiclassical solution into (3.1) and evaluating a determinant over the quadratic fluctuations around the semiclassical solution [25] (the zero mode contribution in the usual way gives a factor it), that from (3.5) we get [5,15,4,26,27]:

$$\hat{H}^o_{eff}(\vec{\tau}) = \Delta_o(S)\hat{\tau}_x \ , \tag{3.10}$$

$$\Delta_o(S) = -\sum_{\eta=\pm} \sqrt{\frac{2}{\pi} Re A_o^{(\eta)}}\Omega_o \exp\{-A_o^{(\eta)}\} \equiv 2\Delta_o \cos \pi S \ , \tag{3.11}$$

$$A_o^{(\eta)} = 2S(K_\parallel/K_\perp)^{1/2} + i\eta\pi S \ , \tag{3.12}$$

where the action $A_o^{(\eta)}$ is that for transition between the two semiclassical minima, either clockwise ($\eta = +$) or anticlockwise ($\eta = -$); the phase $\eta\pi S$ is the Kramers/Haldane phase, coming from the linear in time derivatives kinetic term in (3.2). Without this phase, we would simply have a splitting $|\Delta_o| = \sqrt{2ReA_o/\pi}\Omega_o \exp\{-A_o\}$ with $A_o = 2S(K_\parallel/K_\perp)^{1/2}$.

B. Giant Spin in External Magnetic Field

Let us now include a weak magnetic field ($h = \gamma_e \mid \vec{H}_o \mid /2K_\parallel \ll 1$). The effect of an applied $\vec{H}_o$ is mostly nicely seen in the instanton language; since the 2 possible paths between the degenerate minima involve opposite Haldane topological phase [28,27], this phase can be changed by an external field [29], causing the tunneling splitting to change and even oscillate. Then the corresponding Lagrangian written in terms of angles (θ, φ) has the form (in imaginary time)

$$\begin{aligned} \mathcal{L} &= \mathcal{L}_o + \delta\mathcal{L}_h \\ \delta\mathcal{L}_h &= -\gamma_e S(H_o^x \sin\theta\cos\varphi + H_o^y \sin\theta \sin\varphi + H_o^z \cos\theta) \ , \end{aligned} \tag{3.13}$$

where $\mathcal{L}_o$ was defined in (3.2). As before, we perform the Gaussian integration over the small deviations of φ around zero or π, and obtain the effective Lagrangian for θ. Keeping only linear terms in magnetic field we write

$$\delta\mathcal{L}_h(\theta) = -\gamma_e S(H_o^x \sin\theta + \frac{i\dot{\theta}}{2K_\perp} H_o^y + H_o^z \cos\theta) \ , \tag{3.14}$$

whereas $\mathcal{L}_o(\theta)$ has the form (3.7). With the same accuracy in $h \ll 1$, the correction to the effective action is given by

$$A^{(\eta)} = A_o^{(\eta)} + \int d\tau \delta\mathcal{L}_h(\vec{S}_o^{(\eta)}(\tau)) \ , \tag{3.15}$$

where $\vec{S}_o^{(\eta)}(\tau)$ is the semi-classical trajectory defined by (3.8). Substituting (3.8) in(3.15) we find

$$\delta A_h^{(\eta)} = -\eta\frac{\gamma_e \pi S}{\Omega_o}(\hat{\vec{x}} + i\sqrt{K_\parallel/K_\perp}\hat{\vec{y}}) \cdot \vec{H}_o \ , \tag{3.16}$$

and the final expression for the effective action in the weak magnetic field takes the form [29]

$$A^{(\eta)} = 2S\sqrt{\frac{K_\parallel}{K_\perp}} - \eta\frac{\gamma_e \pi S}{\Omega_o} H_o^x + i\eta\left(\pi S - \frac{\gamma_e \pi S}{\Omega_o}\sqrt{\frac{K_\parallel}{K_\perp}} H_o^y\right) \ , \tag{3.17}$$

If $\vec{H}_o$ is directed along $\hat{\vec{z}}$ (*easy-axis*), this *biases* the symmetric 2-well problem in (1.3). Within our accuracy (we kept only linear terms in $\vec{H}_o$) the correction to the topological phase due to H_o^z iz zero. However if applied along $\hat{\vec{x}}$, the magnetic field lowers the barrier height and displaces the degenerate minima towards each other in the XZ-plane. In this case the clockwise and anticlockwise paths become inequivalent and the tunneling splitting changes with the magnetic field. Application of $\vec{H}_o$ along $\hat{\vec{y}}$ lowers the barrier and distorts the semi-classical path. This field leads to oscillations in the value of the tunneling splitting [29] since the second term in the parentheses is nothing but the Berry phase accumulated by the giant spin during the tunneling.

C. Giant Spin plus Spin Bath

We now include the interaction of the giant spin with the environmental spins. As discussed in section II, we start with the Hamiltonian (1.1) (after dropping V_{dip}), where the $\{\omega_k\}$ are the hyperfine couplings at each site, and the N Pauli variables $\{\vec{\sigma}_k\}$ describe each of the spin-1/2 bath modes. Without the hyperfine term, the total nuclear spectrum, containing $(2)^N$ lines, is almost completely degenerate, with only a tiny spreading $\sim T_2^{-1}$ of levels caused by the internuclear dipolar interaction V_{dip}. With the hyperfine interaction, the nuclear levels are now spread over a total range $\sim \omega_o N$ (assuming $\omega_k \sim \omega_o$ for all nuclei), with most levels concentrated in a Gaussian peak of half-width $\sim \omega_o N^{1/2}$. Since $\omega_o \gg T_2^{-1}$, this means that the nuclear spin spectrum and dynamics are basically *slaved* to the spectrum and dynamics of $\vec{S}$. This of course sharply contrasts with the usual oscillator bath environments, where the bath spectrum is only very weakly perturbed by the coupling to a macroscopic system.

What we wish to do is to truncate to a low energy effective Hamiltonian $H^o_{eff}(\vec{\tau}, \{\vec{\sigma}_k\})$, where $\vec{\tau}$, as before, operates in the subspace of the lowest two levels of $\vec{S}$. The general way to do this is to separate "slow" (frequency $\ll \Omega_o$) from fast (frequency $\gg \Omega_o$) processes, in the combined system/environment dynamics. One then incorporates the fast processes into parameters of the low-energy effective Hamiltonian. In the instanton method, there are two kinds of processes that one may consider, shown schematically in Fig. 2. In the periods between instantons (i.e., when $\vec{n} = \vec{n}_1$ or $\vec{n}_2$), there are *diagonal couplings* between the environment and the system - in general, if one takes into account the bath dynamics, these will be dynamical. On the other hand, the transition between $\vec{n}_1$ and $\vec{n}_2$ (the instanton) can obviously perturb the environment - thus there must, in the reduced Hamiltonian, be a dynamic *non-diagonal* coupling generated between the system and environment. The large values of ω_k mean that *during* the instanton transitions of $\vec{S}$, a great deal can happen in the nuclear bath - the time-varying hyperfine field $\omega_k \vec{S}(\tau)/S$, acting on each $\vec{\sigma}_k$ during the transition, can cause $\vec{\sigma}_k$ to flip. Since one typically has $\omega_k/\Omega_o \ll 1$ (weak coupling regime), the probability that a particular $\vec{\sigma}_k$ will flip during a single instanton passage is $|\alpha_k|^2/2$, where $|\alpha_k| \sim \pi\omega_k/2\Omega_o$ (this result is derived below, in the course of our derivation of H_{eff}; see also refs. [1,3]). Thus in each tunneling transition, roughly $\lambda = 1/2\sum_k |\alpha_k|^2$ nuclear spins flip, and often $\lambda > 1$. Thus in the coupling to the spin bath we must deal with *dynamic* interactions between $\vec{S}$ and the $\vec{\sigma}_k$, during *the instanton itself*, when making the truncation to H_{eff}. These will yield terms non-diagonal in the giant spin basis, in which τ_+ or τ_- may be coupled to several environmental spins at once.

Diagonal coupling: We first deal with the truncated *static* interaction which must exist between $\vec{\tau}$ and the $\{\vec{\sigma}_k\}$ when no tunneling is taking place; this is of necessity a diagonal term. Let the two relevant orientations of $\vec{S}$ are $\vec{S}_1$ and $\vec{S}_2$, with $\vec{S}_1 = -\vec{S}_2$. Then the only interaction with the spin bath is the hyperfine interaction, and the static contribution to the effective Hamiltonian is

$$H^D_{eff} = \frac{1}{2}\hat{\tau}_z \sum_k \omega_k \hat{\sigma}^z_k \ , \tag{3.18}$$

in the reduced Hilbert space.

In the more general case where $\vec{S}_1$ and $\vec{S}_2$ are not antiparallel, we can still define a basis where $|\vec{n}_1\rangle = |\Uparrow\rangle$ and $|\vec{n}_2\rangle = |\Downarrow\rangle$. Now for the two different orientations $\vec{S}_1$ and $\vec{S}_2$, the effective fields acting on $\vec{\sigma}_k$ will be $\vec{\gamma}^{(1)}_k$ and $\vec{\gamma}^{(2)}_k$. These fields are the sums of the hyperfine fields $\omega_k \vec{n}_{1,2}$ and any other static fields acting on the nuclei. We define the *sum* and the *difference* terms as

$$\begin{aligned} \omega^{\|}_k \vec{l}_k &= \vec{\gamma}^{(1)}_k - \vec{\gamma}^{(2)}_k \\ \omega^{\perp}_k \vec{m}_k &= \vec{\gamma}^{(1)}_k + \vec{\gamma}^{(2)}_k \ . \end{aligned} \tag{3.19}$$

where the $\vec{l}_k$ and $\vec{m}_k$ are unit vectors. Then the truncated diagonal interaction takes the form (we project on states $|\Uparrow\rangle$ and $|\Downarrow\rangle$ using standard $(1+\hat{\tau}_z)/2$ and $(1-\hat{\tau}_z)/2$ operators)

$$H^D_{eff} = \sum_{k=1}^{N} \left\{ \vec{\gamma}^{(1)}_k \frac{1+\hat{\tau}_z}{2} + \vec{\gamma}^{(2)}_k \frac{1-\hat{\tau}_z}{2} \right\} \cdot \hat{\vec{\sigma}}_k \equiv \frac{1}{2}\left\{ \hat{\tau}_z \sum_{k=1}^{N} \omega^{\|}_k \, \vec{l}_k \cdot \hat{\vec{\sigma}}_k + \sum_{k=1}^{N} \omega^{\perp}_k \, \vec{m}_k \cdot \hat{\vec{\sigma}}_k \right\} , \tag{3.20}$$

i.e., one term which changes when $\vec{S}_1 \to \vec{S}_2$, and one which does not. Usually $\omega^{\|}_k \gg \omega^{\perp}_k$, and $\omega^{\|}_k \sim \omega_o$.

Non-diagonal coupling: Let us now turn to the dynamic interactions which occur when $\vec{S}$ is tunneling. There are two effects we must deal with - the effect of the nuclear spins on the giant spin dynamics during tunneling, and also the effect of the motion of $\vec{S}$ on the nuclear spins themselves. In general both effects have to be handled together,

in a mutually consistent way. In this paper we concentrate on the weak coupling regime $\omega_k/\Omega_o \ll 1$ when the idea of an effective Hamiltonian is meaningful (we recall that by definition H_{eff} is operating in the low-energy subspace, and that a consistent solution requires $\omega_k \ll \Omega_o$). It is then fairly straightforward to handle interaction effects, in an expansion in ω_k/Ω_o.

Since we want an effective Hamiltonian which describes both $\vec{\tau}$ and the $\{\vec{\sigma}_k\}$, we examine, instead of the transition amplitude $\Gamma^o_{\alpha\beta}$ in (3.1), the more general matrix element

$$\Gamma_{\alpha\beta}(\{\sigma_k^{(\alpha)}, \sigma_k^{(\beta)}\}; t) = \prod_{k=1}^{N} \int_{\vec{\sigma}_k^{(\alpha)}}^{\vec{\sigma}_k^{(\beta)}} \mathcal{D}\vec{\sigma}_k(\tau) \int_{\vec{n}_\alpha}^{\vec{n}_\beta} \mathcal{D}\vec{n}(\tau) exp\left\{ - \int d\tau \big[\mathcal{L}_o(\tau) + \sum_{k=1}^{N} \mathcal{L}_k^o(\tau) + \delta\mathcal{L}_\sigma(\tau) \big] \right\} . \tag{3.21}$$

$$\mathcal{L}_k^o(\tau) = -\frac{i}{2} \dot{\theta}_k \varphi_k \sin\theta_k \tag{3.22}$$

$$\delta\mathcal{L}_\sigma(\tau) = \sum_{k=1}^{N} \vec{\sigma}_k(\tau) \cdot \vec{\gamma}_k(\tau) . \tag{3.23}$$

where $\vec{\gamma}_k(\tau)$ is now the time-dependent field

$$\vec{\gamma}_k(\tau) = \frac{\omega_k \vec{S}(\tau)}{2S} , \tag{3.24}$$

and $\mathcal{L}_o(\tau)$ was defined in (3.2). We assume in this calculation that the instanton is fast and the nuclear dynamics is slow and therefore we first solve for the instanton trajectory minimising $\mathcal{L}_o(\tau) + \delta\mathcal{L}(\tau)$ and calculate then the transition amplitude from $|\vec{n}_\alpha>$ to $|\vec{n}_\beta>$. Since we deal here with non-diagonal matrix elements ($\alpha \neq \beta$), we deal only with the actual transitions, i.e., with the matrix elements $\Gamma_{\Downarrow\Uparrow}$.

The result of such a calculation will depend, of course, on the particular form of the giant spin Hamiltonian, the spin-bath Hamiltonian and the interaction potential. Let us therefore perform the calculation for the easy-axis/easy-plane model (1.3) in zero external magnetic field coupled to the nuclear spins via hyperfine fields. The coupling term (3.23) in the Lagrangian then takes the form

$$\delta\mathcal{L}_\sigma = \sum_{k=1}^{N} \frac{\omega_k}{2} \Big[\sigma_k^x(\tau) \sin\theta\cos\varphi + \sigma_k^y(\tau) \sin\theta\sin\varphi + \sigma_k^z(\tau)\cos\theta \Big] . \tag{3.25}$$

The analogy between this term and (3.13) is obvious. Within the same accuracy, the correction to the minimal action from the hyperfine coupling is given by

$$\delta A_\sigma^{(\eta)} = \sum_{k=1}^{N} \frac{\omega_k}{2} \int d\tau \vec{\sigma}_k(\tau) \cdot \vec{h}_{eff}^{(\eta)}(\tau) = \int d\tau \sum_{k=1}^{N} \delta\mathcal{L}_k^{(\eta)}(\tau) , \tag{3.26}$$

where the instanton-generated field acting on the nuclear spins is defined as

$$\vec{h}_{eff}^{(\eta)}(\tau) = \Big(\eta \sin\theta^{(\eta)}(\tau),\ i\eta\sqrt{K_\parallel/K_\perp} \sin\theta^{(\eta)}(\tau),\ \cos\theta^{(\eta)}(\tau) \Big) , \tag{3.27}$$

For the microscopic nuclear spin 1/2 we do not use a quasiclassical method to evaluate the transition amplitude. Instead, we notice that the problem of evaluating the dynamics of $\sum_k [\mathcal{L}_k^o(\tau) + \delta\mathcal{L}_k^{(\eta)}(\tau)]$ is identical to solving the spin rotation of each of the nuclear spins in the time dependent magnetic field $\omega_k \vec{h}_{eff}(\tau)/2$. The integrals (3.26) are easy to evaluate for the instanton trajectory in the easy-axis/easy-plane model and we find [compare with (3.17)]

$$\delta A_\sigma^{(\eta)} = \eta \sum_{k=1}^{N} \frac{\pi\omega_k}{2\Omega_o} (\hat{\vec{x}} + i\sqrt{K_\parallel/K_\perp}\hat{\vec{y}}) \cdot \vec{\sigma}_k(\tau) . \tag{3.28}$$

A note is in order here. We do not use the Wick rotation from imaginary to real time to calculate the evolution of the microscopic spin wave-function in the time-dependent instanton field $\vec{\gamma}_k(\tau)$. To justify this we consider the

text book solution for a related problem. It is formulated as follows. A spin-1/2 particle passes through a 1-D barrier along the $\hat{\vec{y}}$ - direction. An external magnetic field H_x is nonzero only inside the barrier. What is the spin structure of the transmission coefficient (say in the basis set of eigenfunctions of $\hat{\sigma}_z$)? It is easily shown that one has $T = T_o \exp\{-\alpha\hat{\sigma}_x\}$, where T_o is the transmission coefficient when the external field is zero, and α (which depends on H_x) is *real*. For this reason, we conclude that the co-flip amplitudes have to be calculated in imaginary time, which means that the evolution of the environmental spin does depend on whether the external field acting on it is classical or originates from the tunneling motion of a combined system.

To get the final form of the non-diagonal terms in the effective Hamiltonian we sum up the contributions from the external magnetic field and from the hyperfine coupling to the spin bath and write the result for the transition amplitude as

$$\hat{\Gamma}_{\Downarrow\Uparrow}(t) = it \sum_{\eta=\pm} \sqrt{\frac{2}{\pi} ReA_o}\,\Omega_o \exp\left\{ -A_o^{(\eta)} - i\eta \sum_k \alpha_k \vec{n}\cdot\hat{\vec{\sigma}}_k + i\eta\beta_o \vec{n}\cdot\vec{H}_o \right\} \;; \quad (\Omega_o^{-1} \ll t \ll \Delta_o^{-1}) \;; \tag{3.29}$$

$$\alpha_k \vec{n} = \frac{\pi\omega_k}{2\Omega_o}\big(-i\hat{\vec{x}},\ \sqrt{K_\parallel/K_\perp}\ \hat{\vec{y}}\big) \;; \tag{3.30}$$

$$\beta_o \vec{n} = \frac{\pi\gamma_e S}{\Omega_o}\big(-i\hat{\vec{x}},\ \sqrt{K_\parallel/K_\perp}\ \hat{\vec{y}}\big) \;, \tag{3.31}$$

where $\hat{\Gamma}_{\Downarrow\Uparrow}$ is an operator in the nuclear spin subspace. We may now give the result for the non-diagonal coupling term in this easy-axis/easy-plane model

$$\begin{aligned} H_{eff}^{ND} &= \frac{i}{t}\left[\hat{\tau}_- \hat{\Gamma}_{\Downarrow\Uparrow}(t) + H.c.\right] \\ &= \left[\hat{\tau}_- \Delta_o \sum_\eta \exp\left\{ -i\eta \left(\pi S + \sum_k \alpha_k \vec{n}\cdot\hat{\vec{\sigma}}_k - \beta_o \vec{n}\cdot\vec{H}_o \right) \right\} + H.c.\right] \\ &= 2\Delta_o \hat{\tau}_- \cos\left[\pi S + \sum_k \alpha_k \vec{n}\cdot\hat{\vec{\sigma}}_k - \beta_o \vec{n}\cdot\vec{H}_o \right] + H.c. \;, \end{aligned} \tag{3.32}$$

where $\Delta_o = -\sqrt{2ReA_o/\pi}\ \Omega_o\ e^{-ReA_o}$ as before. Adding the diagonal term (3.20) we get the final truncated effective Hamiltonian:

$$\begin{aligned} H_{eff} = &\left\{ 2\Delta_o \hat{\tau}_- \cos\left[\pi S + \sum_k \alpha_k \vec{n}\cdot\hat{\vec{\sigma}}_k - \beta_o \vec{n}\cdot\vec{H}_o \right] + H.c. \right\} \\ &+ \frac{\hat{\tau}_z}{2} \sum_{k=1}^{N} \omega_k^{\parallel}\, \vec{l}_k \cdot \hat{\vec{\sigma}}_k + \frac{1}{2} \sum_{k=1}^{N} \omega_k^{\perp}\, \vec{m}_k \cdot \hat{\vec{\sigma}}_k \;. \end{aligned} \tag{3.33}$$

with the parameters $\vec{l}_k = \hat{\vec{z}}$, $\omega_k^{\parallel} = \omega_k$, $\omega_k^{\perp} = 0$, for the easy axis/easy plain Hamiltonian (1.3); the parameters α_k, $\vec{n}_k$, and β_o are given in (3.30) and (3.31).

This result for the easy-axis/easy-plane model is not the most general result we can get for the problem of a giant spin coupled to a nuclear spin bath. More generally we will find that both the tunneling splitting Δ_o and the phase πS will be renormalised by the coupling to the nuclear spins - these renormalisations are $O(\omega_k^2/\Omega_o^2)$ for each nuclear spin (they correspond to a change in the instanton trajectory caused by the coupling to the $\{\vec{\sigma}_k\}$, and hence appear first in the 2-nd order in this coupling). Thus more generally we find that $\pi S \to \Phi$, and $\Delta_o \to \tilde{\Delta}_o$, where [2,3]:

$$\Phi = \pi S + \sum_k \phi_k \;, \tag{3.34}$$

$$\tilde{\Delta}_o = \Delta_o \exp\{-\sum_k \delta_k\} \;. \tag{3.35}$$

Physically, the $\{\phi_k\}$ are the Berry phase terms to be added to the instanton phase, coming from the nuclei; and the $\{\delta_k\}$ describe the renormalisation of the tunneling splitting. We do not attempt to calculate either ϕ_k or δ_k here, since their effects are not going to be observable - we only observe $\tilde{\Delta}_o$ and Φ, not Δ_o or the "bare" phase πS.

We have now achieved our main aim in this section, of reducing the giant spin Hamiltonian to a truncated one. It is interesting to notice what kinds of process are now included in this effective Hamiltonian. Notice that if we expand out the cosines in (1.2), we see that we have a whole series of terms like

$$\hat{\tau}_{\pm}\Gamma_{\alpha\beta\gamma\delta\ldots}\hat{\sigma}^{\alpha}_{k_1}\hat{\sigma}^{\beta}_{k_2}\hat{\sigma}^{\gamma}_{k_3}\hat{\sigma}^{\delta}_{k_4}\cdots \ . \tag{3.36}$$

in which the instanton flip of the giant spin couples simultaneously to many *different* nuclear spins. Thus, as well as the simple diagonal and non-diagonal transitions, we also have the possibility (see Fig. 2) of multiple transitions in the bath, stimulated by a single instanton. The parameter $\lambda = \frac{1}{2}\sum_k |\alpha_k|^2$ - as already noted, measures the average number of nuclear spins to be flipped during each instanton.

IV. EXACT DIAGONALIZATION STUDIES.

In this section we wish to verify our analytical derivation (1.2) of H_{eff} by an exact diagonalization method, and to analyse the structure of the low-energy effective Hamiltonian for arbitrary values of parameters S and $K_{\perp}/K_{\parallel}$, including regimes where the WKB approach breaks down.

For simplicity we consider the Hamiltonian for a giant spin coupled to a single nuclear spin 1/2 (for small ω_k/Ω_o nuclear spin contributions are *additive*); a similar tactic was employed by Abarenkova and Angles d'Auriac [17]. We have

$$H(\vec{S},\vec{\sigma}) = \frac{1}{S}\Big[-S_z^2 + \Lambda S_y^2 + \frac{\omega_o}{2}\vec{S}\cdot\vec{\sigma}\Big] - \vec{H}_o\vec{S}\ , \tag{4.1}$$

where we measure energy in units of $K_{\parallel}$, magnetic field in units $K_{\parallel}/\gamma_e$, and we define the anisotropy parameter $\Lambda = K_{\perp}/K_{\parallel}$. Let us also apply the magnetic field $\vec{H}_o$ along the $\hat{\vec{y}}$ axis (i.e., $\vec{H}_o = \vec{H}_y$). For this particular choice of the external parameters we can rewrite (1.2) as follows

$$H_{eff} = \left\{ 2\Delta_o\hat{\tau}_- \cos\left[\pi S - \psi + \alpha\vec{n}\cdot\hat{\vec{\sigma}}\right] + H.c.\right\} + \frac{\omega_o}{2}\hat{\tau}_z\cdot\hat{\sigma}_z + \frac{\omega_o H_y}{4\Lambda}\hat{\sigma}_y\ , \tag{4.2}$$

where the last two terms describe the static diagonal interaction (and as before, we neglect both the interaction between the nuclear spin and magnetic field, and the internuclear dipolar coupling). In this equation we have defined

$$\alpha\vec{n} = \frac{\pi\omega_o}{2\Omega_o}\big(-i\hat{\vec{x}},\ \hat{\vec{y}}/\sqrt{\Lambda}\big)\ , \tag{4.3}$$

$$\psi = \frac{\pi S H_y}{2\Lambda}\ . \tag{4.4}$$

Let us start by defining the diagonalization procedure. Since the giant spin only weakly couples to the nuclear spin 1/2, we have four lowest energy levels, well-separated from higher levels by the instanton frequency Ω_o. The Hamiltonian (4.2) is given in the Hilbert space of these four levels. Therefore, we can write

$$\langle a|H_{eff}|b\rangle \approx \langle a|H|b\rangle\ ; \quad (a\ , b = 1\ , \ldots\ , 4) \tag{4.5}$$

or

$$\langle a|H_{eff}|b\rangle \approx \langle a|\sum_{\gamma=1}^{4} E_\gamma|\Psi_\gamma\rangle\langle\Psi_\gamma|b\rangle = \sum_{\gamma=1}^{4}(\hat{U}^{+})_{a\gamma}E_\gamma\hat{U}_{\gamma b}\ , \tag{4.6}$$

where

$$\hat{U}_{\gamma b} = \langle\Psi_\gamma|b\rangle \tag{4.7}$$

and the $|\Psi_\gamma\rangle$ are the four eigenfunctions of the Hamiltonian (4.1), corresponding to the four lowest energy levels $E_1\,, ...\,, E_4$. In fact, Eq. (4.5) is nothing but the definition of the effective Hamiltonian.

The choice of the appropriate basis set of $|a\rangle$ is important here. The most convenient and physically transparent basis set is that of the noninteracting system, i.e. the eigenfunctions of $H = H_0(\vec{S})$. Let $|\Phi_1^o\rangle$ and $|\Phi_2^o\rangle$ be the eigenfunctions corresponding to the two lowest levels of H_o for the giant spin $\vec{S}$. Then the functions

$$|\chi_\pm\rangle = \frac{|\Phi_1^o\rangle \pm |\Phi_2^o\rangle}{\sqrt{2}} \tag{4.8}$$

are localised single-well states, which in the semiclassical limit correspond to the previously introduced $|\vec{n}_1\rangle$ and $|\vec{n}_2\rangle$. With nuclear spins added we define the basis set $|a = 1, 2, 3, 4\rangle$ as

$$|1\rangle = |\chi_+\rangle \otimes \begin{pmatrix}1\\0\end{pmatrix}\,,\;\; |2\rangle = |\chi_+\rangle \otimes \begin{pmatrix}0\\1\end{pmatrix}\,,\;\; |3\rangle = |\chi_-\rangle \otimes \begin{pmatrix}1\\0\end{pmatrix}\,,\;\; |4\rangle = |\chi_-\rangle \otimes \begin{pmatrix}0\\1\end{pmatrix} \tag{4.9}$$

(where $\otimes$ stands for the direct product of state vectors). This particular choice of the basis set $|\alpha\rangle$ is the starting point for our diagonalization procedure.

The diagonalization procedure itself is arranged as follows. First, one calculates the eigenstates of the noninteracting problem to construct the set $|a\rangle$, and then diagonalizes the interacting Hamiltonian to obtain the energy spectrum and the unitary transformation $\hat{U}$ as defined in Eqs. (4.6) and (4.7). As H_{eff} is a matrix (4×4) matrix it can be written as

$$H_{eff} = \sum_{i,j=0}^{3} C_{ij} \cdot \hat{\tau}_i \otimes \hat{\sigma}_j\;, \tag{4.10}$$

where $\hat{\tau}_i$ and $2 \cdot \hat{\sigma}_i$ $(i = 1, 2, 3)$ are the Pauli matrices and $\hat{\tau}_o$, $\hat{\sigma}_o$ are the unit matrixes. Thus

$$C_{ij} = Tr\{H_{eff} \cdot (\hat{\tau}_i \otimes \hat{\sigma}_j)\}\;. \tag{4.11}$$

We analyse these coefficients and compare them with those resulting from (4.2). If S is an integer we get (we omit here the $\otimes$ sign)

$$\begin{aligned} H_{eff} \approx (-1)^S \left\{ 2\Delta_o \cos\psi \cdot \hat{\tau}_x\hat{\sigma}_o - 2\Delta_o\alpha \sin\psi \cdot \hat{\tau}_y\hat{\sigma}_x + 2\Delta_o \frac{\alpha}{\sqrt{\Lambda}} \sin\psi \cdot \hat{\tau}_x\hat{\sigma}_y \right\} \\ + \frac{\omega_o}{2}\hat{\tau}_z\hat{\sigma}_z + \frac{\omega_o H_y}{4\Lambda}\hat{\tau}_o\hat{\sigma}_y\;; \qquad \alpha = \frac{\pi\omega_o}{2\Omega_o}\;, \end{aligned} \tag{4.12}$$

and for $S = 1/2$-integer we get

$$\begin{aligned} H_{eff} \approx (-1)^{2S+1} \left\{ 2\Delta_o \sin\psi \cdot \hat{\tau}_x\hat{\sigma}_o + 2\Delta_o\alpha \cos\psi \cdot \hat{\tau}_y\hat{\sigma}_x - 2\Delta_o \frac{\alpha}{\sqrt{\Lambda}} \cos\psi \cdot \hat{\tau}_x\hat{\sigma}_y \right\} \\ + \frac{\omega_o}{2}\hat{\tau}_z\hat{\sigma}_z + \frac{\omega_o H_y}{4\Lambda}\hat{\tau}_o\hat{\sigma}_y\;. \end{aligned} \tag{4.13}$$

Now we turn to the results.

(a) Semiclassical regime S $\gg$ 1: We start by carrying out the numerical analysis for a wide region of parameters S and Λ and as an example we present our results for $S = 50$, $\Lambda = 50$, and $\omega_o = 0.2$ (recall again that energy is measured in units of $K_\parallel$). In full agreement with (4.12) the effective Hamiltonian H_{eff}^{ED}, derived by the exact diagonalization, has only five non-zero coefficients C_{ij}, i.e.,

$$H_{eff}^{ED} = C_{xo} \cdot \hat{\tau}_x\hat{\sigma}_o + C_{xy} \cdot \hat{\tau}_x\hat{\sigma}_y + C_{yx} \cdot \hat{\tau}_y\hat{\sigma}_x + C_{oy} \cdot \hat{\tau}_o\hat{\sigma}_y + C_{zz} \cdot \hat{\tau}_z\hat{\sigma}_z\;. \tag{4.14}$$

In Fig. 4 we present the behavior of the 4 non-diagonal coefficients as functions of the magnetic field H_y, and compare with the corresponding analytical forms (4.12), coming from the instanton analysis. As to the value of C_{zz}, numerically it is 0.0972 in comparison with the analytical result 0.1, showing a small zero point vibration (z.p.v) reduction of $\langle\chi_+|\hat{S}_z|\chi_+\rangle < S$.

We also have performed calculations for half-integer spins. For $S = 49.5$, $\Lambda = 49.5$, and $\omega_o = 0.2$, for example, we have found a similarly good agreement between the numerical and analytical (4.13) results.

Bearing in mind that we kept only the leading terms in the hyperfine coupling when deriving (4.12, 4.13) we conclude from these results that the effective Hamiltonian (4.2) (and (1.2)) gives a complete description of the low-energy dynamics of the system in weak magnetic field for $S \gg 1$, and that moreover the values of the coefficients computed for the effective Hamiltonian by the instanton expansion are in rather good agreement with the exact results.

(b) Beyond WKB: Arbitrary values of S and Λ: Although the above results strongly support the validity of our effective Hamiltonian (1.2) for $S \gg 1$, it is of considerable interest to explore its validity when we are far from this WKB limit. In fact it was shown in the original papers of van Hemmen et al., as well as Enz and Schilling [4], that WKB results for the *free* giant spin are remarkably accurate even when S is less than 10, at least as far as the calculation of tunneling splittings are concerned. Thus we shall now use our exact diagonalisation results to tell us how accurate is our H_{eff} in (1.2), when S and Λ are arbitrary, and the action A_o is not much larger than unity.

We begin by defining a function $\Psi(S, \Lambda, H_y)$, such that the actual tunneling splitting $\Delta_o(\Psi) = \Delta_o \cos\Psi$ for the non-interacting problem (for S-integer). In the semiclassical limit $\Psi = \psi$; we wish to see deviations for small S and large Λ. Notice that even for small values of S, the coefficient C_{x0} in (4.14) still oscillates with H_y like $cos\Psi$ (and C_{xy} and C_{yx} like $\pm \sin\Psi$).

In Fig. 5 we present our numerical results for Ψ/ψ as a function of S and Λ, with H_y^o equal to some value smaller than one period of oscillation of $\Delta_o(\Psi)$ [in fact, in most cases $\Psi \sim H_y$ rather precisely unless $S < 3$]. We plot the ratio Ψ/ψ as a function of S at $\Lambda = 50$ and $\Lambda = 10$ (Fig. 5.a) and as a function of Λ at $S = 50$ (Fig. 5.b) to see where the analytical prediction (4.4) becomes invalid. As we can see from Fig. (5.a), the difference between the exact value of Ψ and the semiclassical result $\Psi = \psi$ occurs at small values of S, whereas for $S > 10$ this difference has almost disappeared. Moreover, the curve at $\Lambda = 10$ is falling to 1 more rapidly than at $\Lambda = 50$, because with increasing effective action A_o the WKB description becomes more accurate. Fig.(5.b) shows the violation of the WKB regime with increase of Λ at $S = 50$ as the effective action A_o goes down. At $S = 50$ the analytical formula (4.4) for ψ begins to show appreciable deviations from the exact result once $\Lambda \geq 700$.

So far so good; we now turn to the analysis of the interaction Hamiltonian itself, by considering the dependence of the coefficient α on S and Λ. First, we calculate α as a function of S at a constant value of the effective action A_o. One expects that for large A_o there should be good agreement between the numerical result and the analytical result (4.3). In Fig. 6 we plot the coefficient C_{yx}, divided by $2\Delta_o \sin\Psi$, together with α, defined in (4.3), vs the giant spin quantum number S at $\Lambda = S^2/50$. With this definition of Λ the effective action A_o is a constant ≈ 14. Since Δ_o and $\Psi(S, \Lambda, H_y^o)$ are already known numerically, we plot the results of the exact diagonalization for α together with the analytical one. From Fig.6 we see that once $S \geq 10$, the result (4.3) for the effective coupling α is extremely good.

To study the deviations from (4.3), we show in Fig.7 numerical results for $C_{yx}/(2\Delta_o \sin\Psi)$ together with α from (4.3) vs the giant spin quantum number at $\Lambda = 50$ and $\Lambda = 10$ (Fig. 7(a)) and vs Λ at $S = 50$ and $S = 10$ (Fig. 7(b)). The solid lines in Fig. 7(a) (parallel to the S-axis) are the analytical results. We can see, that at small values of the giant spin (at $S \leq 10$ in this particular case) it becomes useful to derive numerical results to describe its interaction with the nuclear spin. Notice (Fig. 7(b)) that the numerical (triangles) and analytical (solid) curves coincide extremely well for $S = 50$ whereas for $S = 10$ the differences between the numerical and analytical curves become obvious once $\Lambda \geq 100$.

Thus we can conclude that (4.3) becomes more and more accurate with the increase of S at any fixed value of Λ once the effective action $A_o = 2S/\Lambda^{1/2}$ becomes significantly greater than unity (compare, e.g., in Fig. 7(b), the point $\Lambda = 500$ for $S = 10$ (triangles down), where the effective action $A_o < 1$, with the point having the same value of Λ, but $S = 50$, for which $A_o > 1$.

Finally we analyse the effect of z.p.v. of the giant spin on the value of the diagonal coupling. The orientation of the giant spin is fluctuating around the classical energy minima, resulting in a reduction of the static diagonal interaction. It is easy to see from (3.7) that the value of $< \sin^2\theta > \approx 1/A_o$. From this it follows that the coefficient $\omega_o^{\|}$ in the longitudinal diagonal interaction (ie., that proportional to $\hat{\tau}_z \cdot \hat{\sigma}_z$ in (4.2)), can be corrected by replacing $\omega_o \Rightarrow \omega_o(1 - 1/A_o)^{1/2}$. Thus, with increasing Λ, the giant spin becomes more and more "delocalized", and the extent of the delocalisation is parametrized in the exact diagonalisation results by the z.p.v. reduction of C_{zz}. To show how accurate is the simple replacement $\omega_o \to \omega_o(1 - 1/A_o)^{1/2}$, we compare in Fig.8 the coefficient $2C_{zz}/\omega_o$ against $(1 - 1/A_o)^{1/2}$, both plotted as functions of S at $\Lambda = 50$ (triangles up) and at $\Lambda = 10$ (triangles down).

(c) Zero magnetic field: Nonlinear corrections in α: Our instanton derivation in section III was carried out only as far as 1st-order in the effective coupling α_k. However we see immediately that in (4.2), when S =integer and in zero external field, the nondiagonal term is affected by the coupling only in the second order in α, i.e., $\Delta_o \cosh(\alpha) \approx \Delta_o(1 + \alpha^2/2)$. As discussed above [see Eq. (3.35)] in a consistent calculation one may also have

corrections $\sim \alpha^2$ which are not accounted for in Eq. (4.2). To find these corrections we have performed the necessary numerical calculations for for integer and half-integer S in zero external field.

In Fig.9(a) we show the behavior of the coefficient $C_{xo}/2\Delta_o$ (or tunneling splitting renormalisation) vs α for integer S. Our analysis shows that the behavior of C_{xo} in the region $0 \leq \alpha \leq 0.5$ is very close to $2\Delta_o(1-\alpha^2/2)$. These results suggest that the parameter δ in Eq. (3.35) is given by α^2, and the nonlinear correction may be accounted for by substituting $\Delta_o \Rightarrow \Delta_o(\alpha) = \Delta_o(1-\alpha^2)$ in the effective Hamiltonian (4.2). In Fig 9(a) we plot the numerical results for $C_{xo}/2\Delta_o$ (triangles up) together with the analytical approximation $(1-\alpha^2)\cosh(\alpha)$ (solid line). All other coefficients C_{ij} (except C_{zz}) are zero.

To see whether the ansatz $\Delta_o \Rightarrow \Delta_o(\alpha)$ really works well, we considered also the case of half-integer S. In Fig.9(b) we plot the coefficient $C_{yx}/2\Delta_o$ vs α (triangles up) together with the analytical approximation $(1-\alpha^2)\sinh(\alpha)$ (solid line). As we can see from this figure, our approximation works quite well in the region $0 \leq \alpha \leq 0.5$.

This completes our numerical analysis of the low-energy effective Hamiltonian in the problem of the giant spin coupled to the spin enviroment. Our main conclusion in this section can be formulated as follows: the predictions about the low-energy dynamics of the system in the magnetic field, given by (4.2) (and (1.2) correspondingly), are rather accurate when the effective action $A_o > 1$.

V. CONCLUSION.

To conclude, it may be useful to summarize some of the esential mathematical features of our analysis. We started with a "high-energy" form for the central spin coupled to its spin bath environment, given by (1.1). This was truncated to the low-energy form (1.2) by an instanton-type procedure. However the results of this truncation were different from the usual quantum environment models, mainly because the spin bath modes are strongly coupled to the central spin. As a consequence much of the physics of the problem is contained in dynamic non-diagonal terms (in contrast to the oscillator bath models, where such terms are almost irrelevant), as well as in almost static but very strong diagonal couplings. The instanton derivation also allows one to evaluate the coefficients in the low-energy effective Hamiltonian, for a given initial "high-energy" Hamiltonian for a giant spin coupled to a nuclear spin bath.

In the present paper we set out to find out how accurate this instanton result for the low-energy effective Hamiltonian really is. Using an exact diagonalisation procedure, we were not only able to verify that the effective Hamiltonian is correct, but also that the coefficients in it are rather accurately given by the "first-order" (in ω_k/Ω_o) instanton expansion, provided we are working in the regime where the semiclassical WKB approximation works.

The importance of this result is simply that the low-energy effective Hamiltonian, in the form we have given, turns out to be remarkably easy to use in practical calculations of the spin dynamics of the central spin, as we have shown in a number of other papers (see, eg., ref. [16], and refs therein). From the present calculations we now have a good idea of how trustworthy these calculations are- essentially they are as good as the semiclassical approximation itself.

VI. ACKNOWLEDGEMENT

This work was supported by NSERC in Canada and by the Russian Foundation for Basic Research (grant 97-02-16548). We would like to thank B.G. Turrell for some very helpful discussions, and also V. Kashurnikov for his help in writting of the exact diagonalization code. We also thank the Institute for Nuclear Theory at the University of Washington for its hospitality and the Department of Energy for partial support during the completion of this work.

FIGURE CAPTIONS

Figure 1 A typical trajectory for S_z, contributing to the path integral for the propagator of a free giant spin. The time scale for "fast" variations of S_z while it is in one of the 2 wells or making a transition between the weells is Ω_o^{-1}, whereas the time between jumps (instantons) is much longer, roughly Δ_o^{-1}.

Figure 2 Processes which may occur when a 2-state system is coupled to some background environment - we show some possible kinds of coupling between the path of the 2-state system (solid line) and the environment. There is a diagonal coupling (ie., a coupling to τ_z), indicated by "D", to a single environmental mode (whose propagator is indicated by a wavy line). The first non-diagonal coupling (labelled by "ND") is to a *single* environmental mode, whereas the second one couples simultaneously to 3 different environmental modes.

Figure 3 Processes occuring in the propagator for a 2-state system coupled to a set of oscillator modes, after one averages over these modes ("integrates them out"), which allows us to join the wavy lines of the previous figure in the usual way. Process (a) involves the excitation of an environmental mode when the central spin is in state $|\Uparrow>$, and with re-absorption when it is in state $|\Downarrow>$; process (b) has the central spin in the same state for both emission and re-absorption. Both these processes involve only diagonal operators. Process (c) involves non-diagonal terms, and process (d) involves both diagonal and non-diagonal terms.

Figure 4 The numerical coefficients C_{ij} (4.11) of the effective Hamiltonian (4.14) in comparison with the analytical expressions from (4.12). The figures are: (a) C_{x0} (solid line) and $2\Delta_o \cos\psi$ (dashed line), (b) C_{xy} (solid line) and $2\Delta_o \alpha \sin\psi/\Lambda^{1/2}$ (dashed line), (c) C_{yx} (solid line) and $2\Delta_o \alpha \sin\psi$ (dashed line), (d) C_{y0} (solid line) and $\omega_o H_y/4\Lambda$ (dashed line); $S = 50, \Lambda = 50, \omega_o = 0.2$.

Figure 5 The ratio $\Psi(S, \Lambda, H_y^o)/\psi$ of the exact phase Ψ to the weak-field expression for ψ (4.4): (a) vs the giant spin quantum number S at $\Lambda = 50$ (triangles up) and at $\Lambda = 10$ (triangles down), (b) vs Λ at $S = 50$ (triangles up); $\omega_o = 0.1$, $H_y^o = \Lambda/8S$.

Figure 6 The numerical coefficient $C_{yx}/(2\Delta_o \sin\Psi)$ (triangles up) together with the analytical co-flip amplitude α from (4.3) (solid line) at $\Lambda = S^2/50$; $\omega_o = 0.1$, $H_y^o = \Lambda/8S$.

Figure 7 The deviation of α from the analytical expression (4.3). The figures are: (a) The numerical coefficient $C_{yx}/(2\Delta_o \sin\Psi)$ at $\Lambda = 50$ (triangles up) and at $\Lambda = 10$ (triangles down) together with the analytical α from (4.3) (solid lines) vs the giant spin quantum number S, (b) The numerical coefficient $C_{yx}/(2\Delta_o \sin\Psi)$ at $S = 50$ (triangles up) and at $S = 10$ (triangles down) together with the analytical α (solid line) vs Λ; $\omega_o = 0.1$, $H_y^o = \Lambda/8S$.

Figure 8 The numerical coefficient $C_{zz}/0.5 \cdot \omega_o$, vs the giant spin S at $\Lambda = 50$ (triangles up) and at $\Lambda = 10$ (triangles down); $\omega_o = 0.1$, $H_y^o = \Lambda/8S$.

Figure 9 Zero magnetic field: (a) The numerical coefficient $C_{x0}/2\Delta_o$ vs α at $S = 50$ and $\Lambda = 50$ (triangles up) together with the analytical approximation $(1 - \alpha^2)\cosh(\alpha)$ (solid line); (b) The numerical coefficient $C_{yx}/2\Delta_o$ vs α (triangles up) at $S = 49.5$ and $\Lambda = 49.5$ together with the analytical approximation $(1 - \alpha^2)\sinh(\alpha)$ (solid line).

---

[1] P.C.E. Stamp, Nature, **359**, 365 (1992); Proc. LT-20 Conf. (August, 1993; Eugene, Oregon), published in Physica **B197**,133 (1994); see also UBC Preprint (Sept. 1992), unpublished.

[2] N.V. Prokof'ev and P.C.E. Stamp, J. Phys. CM Lett. **5**, L663-L670 (1993).

[3] N.V. Prokof'ev and P.C.E. Stamp,*"Spin Environments and the Suppression of Quantum Coherence"*, Chapter in [6], 347-371.

[4] J.L. van Hemmen and S. Suto, Europhys. Lett. **1**, 481 (1986), and Physica **B141**, 37 (1986); M.Enz and R. Schilling, J. Phys. **C19**, L711 (1986); and *ibid.* 1765 (1986). See also J.L. van Hemmen and W.F. Wreszinski, Comm. Math. Phys. **119**, 213 (1988); and J.L. van Hemmen and S. Suto, Proc. NATO Conf. in Chichilienne, France, June 1994; to be published as *"Theory of Mesoscopic Quantum Tunneling in Magnetism: a WKB Approach"*, Chapter in [6].

[5] E.M. Chudnovsky and L. Gunther, Phys. Rev. Lett. **60**, 661 (1988).

[6] *"Quantum Tunneling of Magnetisation-QTM'94"*, Proc NATO workshop, Chichilienne, June 1994 (ed. L. Gunther, B. Barbara, Kluwer publishing, 1995), contains a large selection recent reviews of different aspects of the field of Quantum Nanomagnetism.

[7] D.D. Awschalom et al., Science **258**, 414 (1992), and refs. therein.

[8] J. Villain et al., Europhys. Lett., **27**, 159 (1994), and refs. therein.

[9] S. Sachdev and R.N. Bhatt, Phys. Rev. **34**, 4898 (1986); and J. Appl. Phys. **61**, 4366 (1987).

[10] T. Kasuya, A. Yanase, Rev. Mod. Phys. **40**, 684 (1968); for recent work, see T. Dietl et al., Phys. Rev. Lett. **74**, 474 (1995), and refs. therein.

[11] See, e.g., S. Sachdev, Physics World **7**, 25 (1994), and refs. therein; C.T. Muruyama, W.G. Clark, and J.Sanny, Phys. Rev. **B29**, 6063 (1984).

[12] M. Gaudin, J. de Physique **37**, 1087 (1976); and "La fonction d'onde de Bethe" (Masson, collection de CEA; Paris, 1983).

[13] A.O. Caldeira and A.J. Leggett, Ann. Phys. (N.Y.), **149**, 374 (1983); see also A.J. Leggett *et al.*, Rev. Mod. Phys. **59**, 1 (1987).
[14] P.C.E. Stamp, Phys. Rev. Lett., **61**, 2905 (1988).
[15] P.C.E. Stamp, E.M. Chudnovsky, and B. Barbara, Int. J. Mod. Phys. **B6**, 1355-1478 (1992).
[16] N.V. Prokof'ev, P.C.E. Stamp, J. Low Temp. Phys., **104**, 143 (1996).
[17] N. Abarenkova and J.-C. Angles d'Auriac, Phys. Lett., A, **219**, 335 (1996).
[18] B. Barbara and E.M. Chudnovsky, Phys. Lett. **A145**, 205 (1990).
[19] I.V. Krive and O.B. Zaslavskii, J. of Phys. CM, **2**, 9457 (1990).
[20] G. Tatara and H. Fukuyama, Phys. Rev. Lett. **72**, 772 (1994), and J. Phys. Soc. Japan **63**, 2538 (1994).
[21] A. Garg and G.H. Kim, Phys. Rev. Lett. **63**, 2512 (1989).
[22] E.M. Chudnovsky, Phys. Rev. Lett. **72**, 3433 (1994).
[23] P.C.E. Stamp, Phys. Rev. Lett., **66**, 2802 (1991).
[24] N.V. Prokof'ev, P.C.E. Stamp, Submitted to Nature (1996).
[25] C. Callan and S. Coleman, Phys. Rev. D**15**, 2929 (1977); Phys. Rev. D**16**, 1762 (1977).
[26] A.S. Ioselevich, JETP Lett. **45**, 571 (1987).
[27] J. von Delft and C. Henley, Phys. Rev. Lett., **69**, 3236 (1992); D. Loss, D.P. di Vincenzo, and G. Grinstein, Phys. Rev. Lett., **69**, 3232 (1992).
[28] F.D.M. Haldane, Phys. Rev. Lett. **50**, 1153 (1983).
[29] E.N. Bogachek and I.V. Krive, Phys. Rev. B, **46**, 14559 (1992).

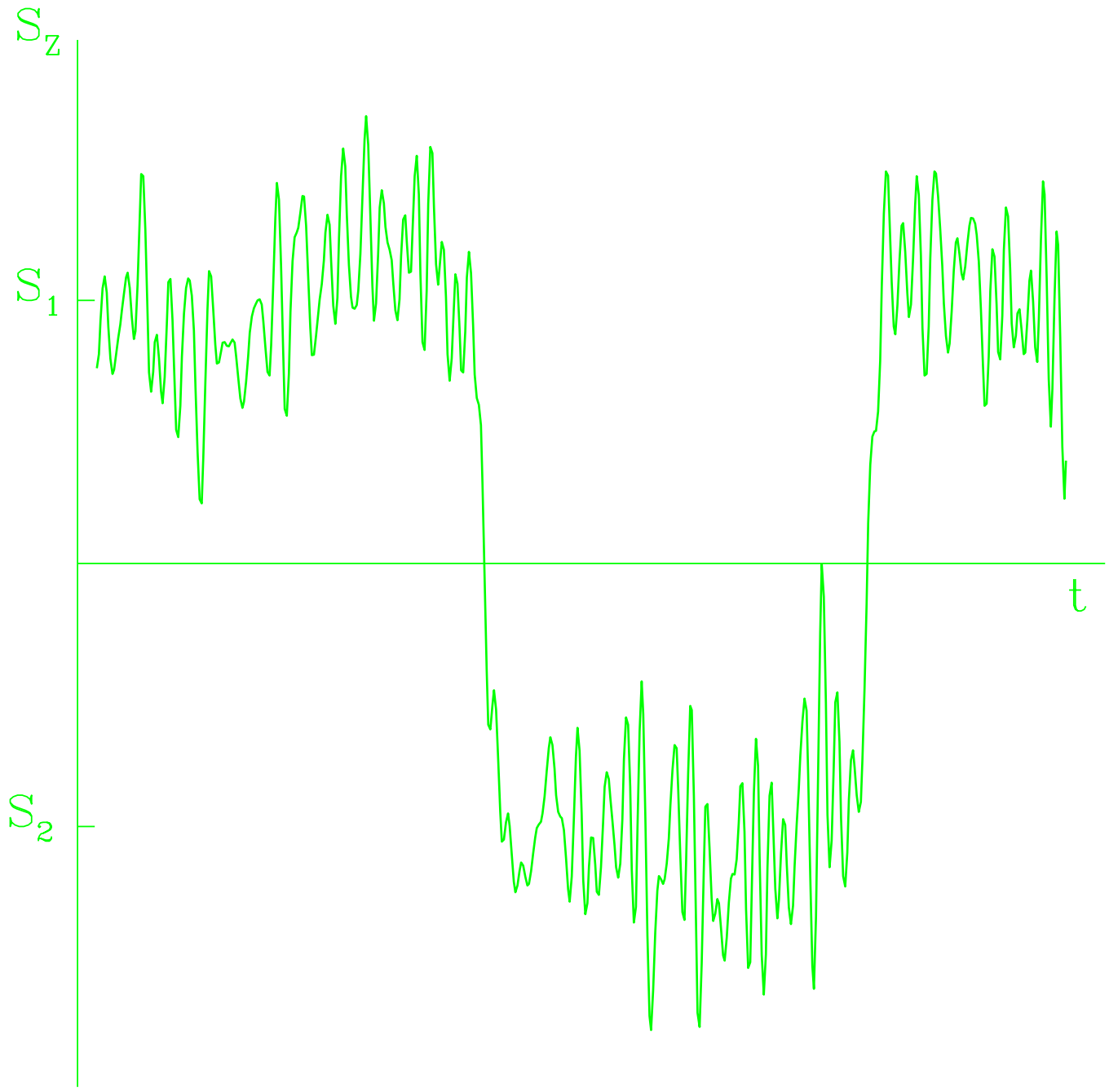
S_z
S_1
S_2
t

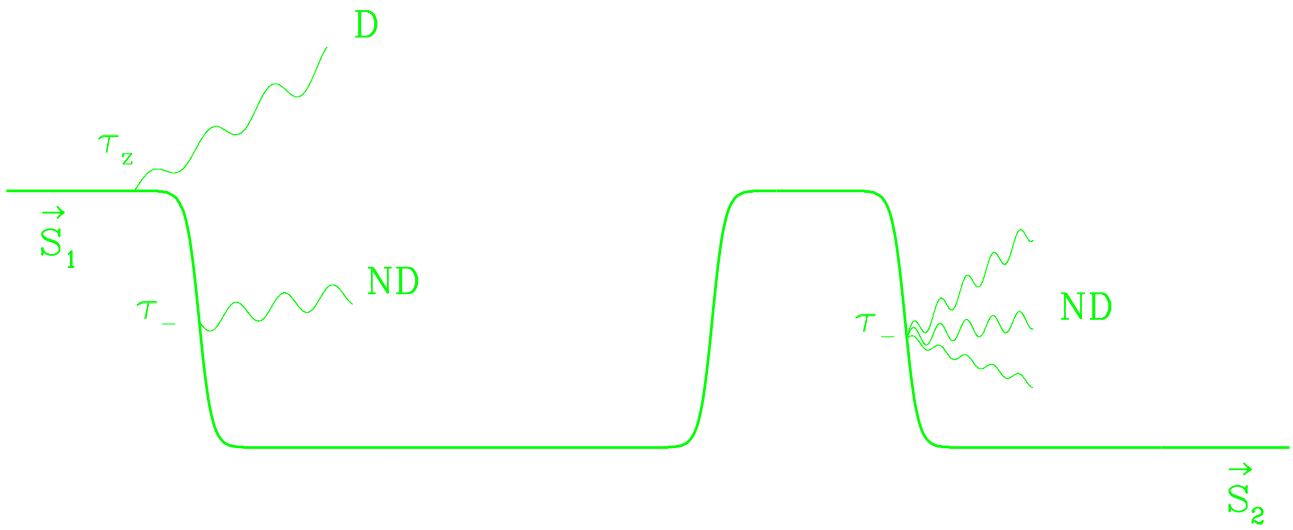
D
τ_z
$\vec{S}_1$
ND
τ_-
τ_-
ND
$\vec{S}_2$

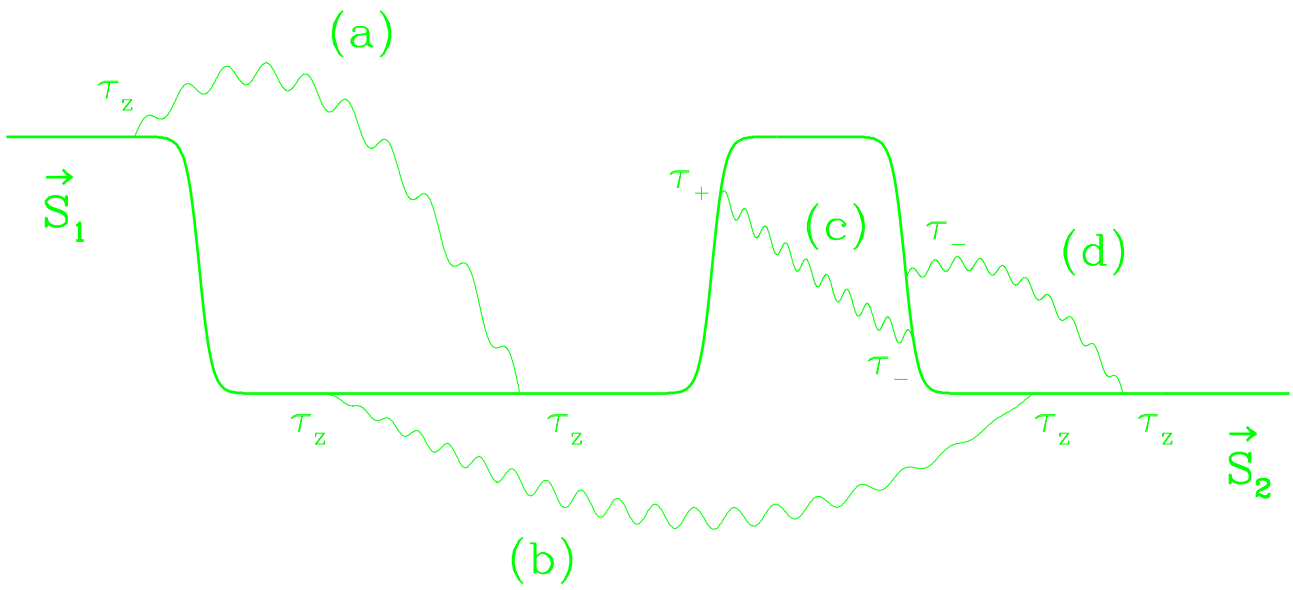
(a)
τ_z
$\vec{S}_1$
τ_+
(c)
τ_-
(d)
τ_-
τ_z
τ_z
τ_z
τ_z
$\vec{S}_2$
(b)

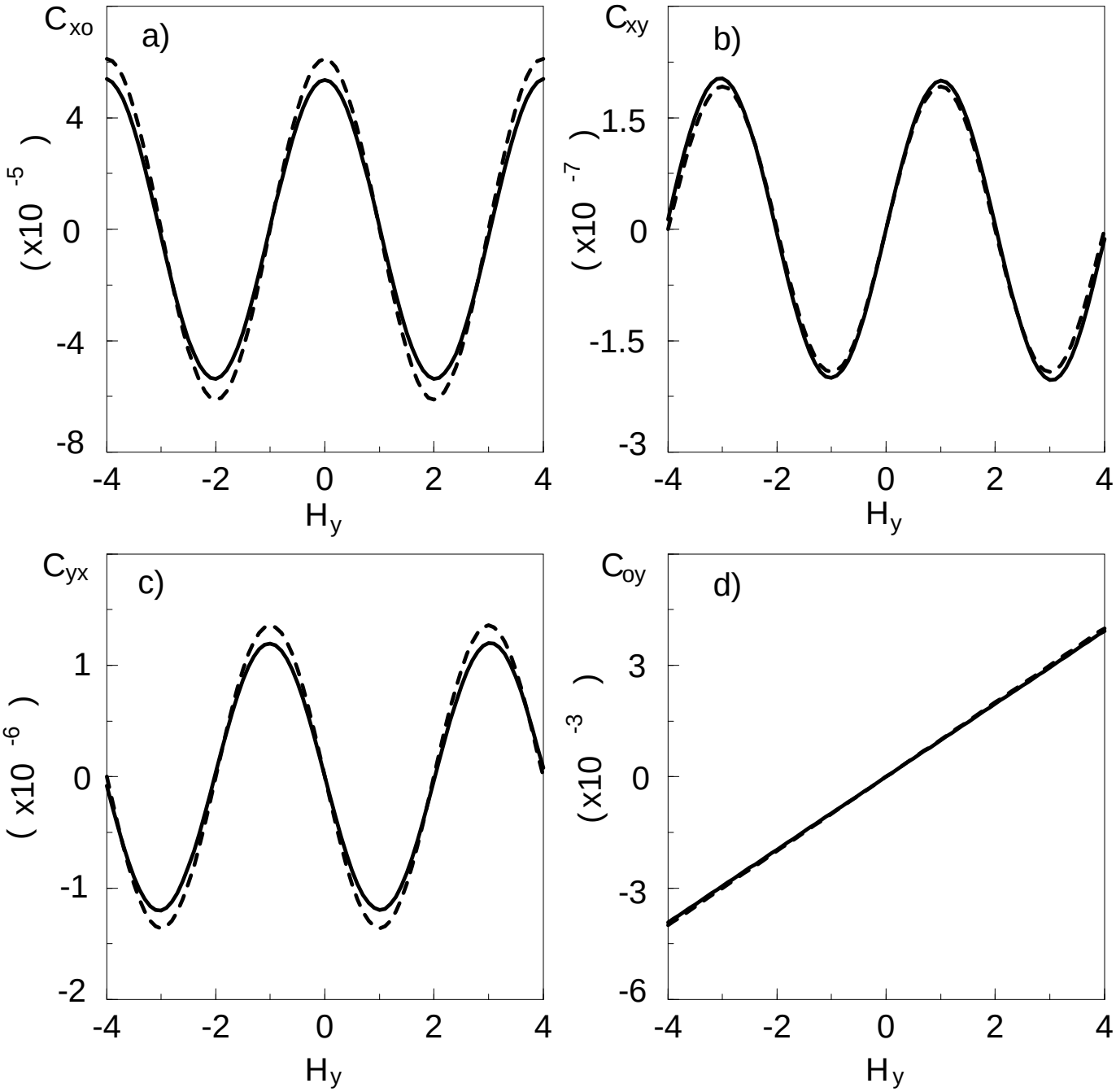
a)
C_{xo}
(x10 $^{-5}$)
4
0
-4
-8
-4
-2
0
2
4
H_y
b)
C_{xy}
(x10 $^{-7}$)
1.5
0
-1.5
-3
-4
-2
0
2
4
H_y
c)
C_{yx}
(x10 $^{-6}$)
1
0
-1
-2
-4
-2
0
2
4
H_y
d)
C_{oy}
(x10 $^{-3}$)
3
0
-3
-6
-4
-2
0
2
4
H_y

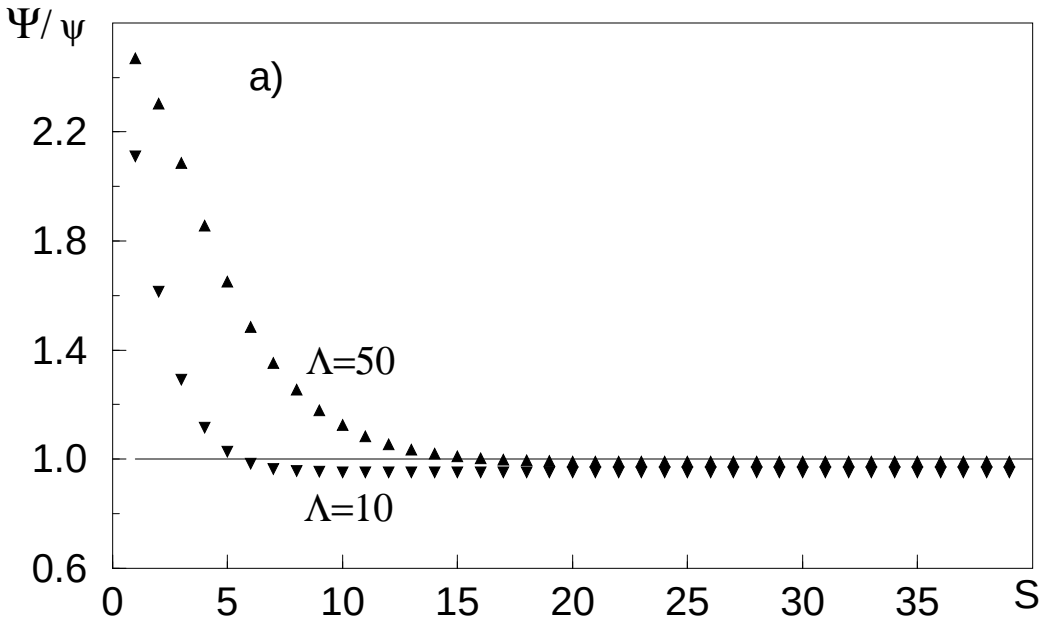
Ψ/ψ
a)
2.2
1.8
1.4
1.0
0.6
Λ=50
Λ=10
0
5
10
15
20
25
30
35
S

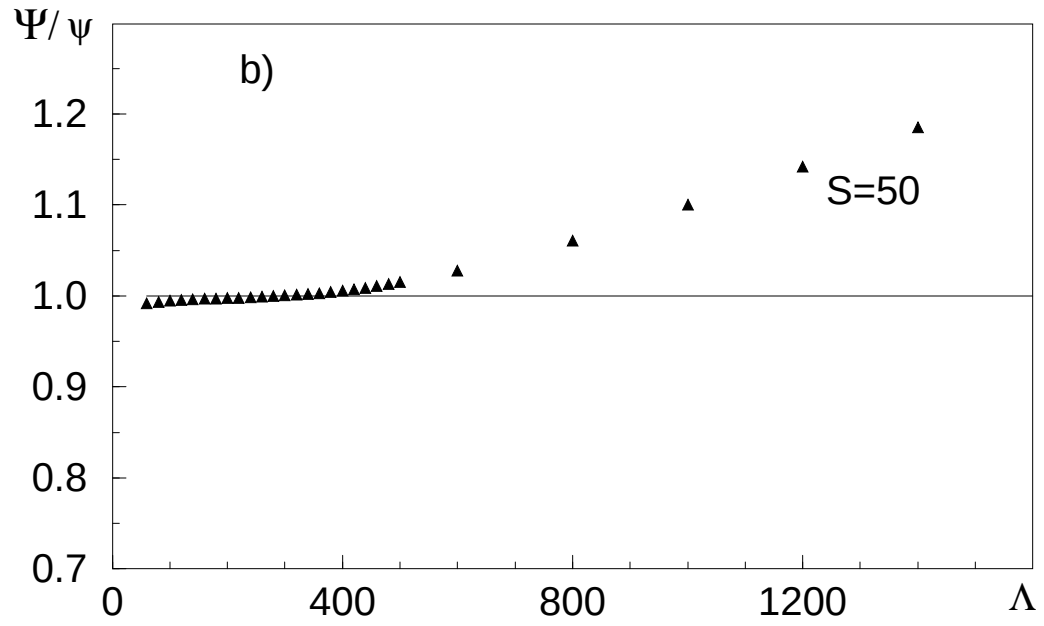
Ψ/ψ
b)
1.2
1.1
1.0
0.9
0.8
0.7
S=50
0
400
800
1200
Λ

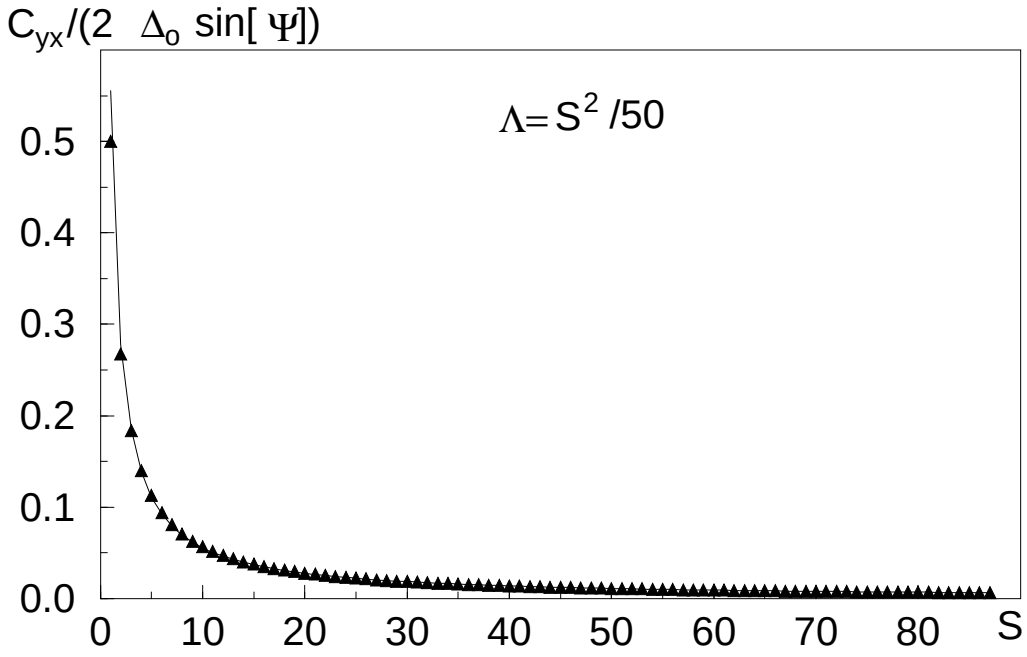
$C_{yx}/(2\ \Delta_o \sin[\Psi])$
$\Lambda = S^2/50$
0.5
0.4
0.3
0.2
0.1
0.0
0
10
20
30
40
50
60
70
80
S

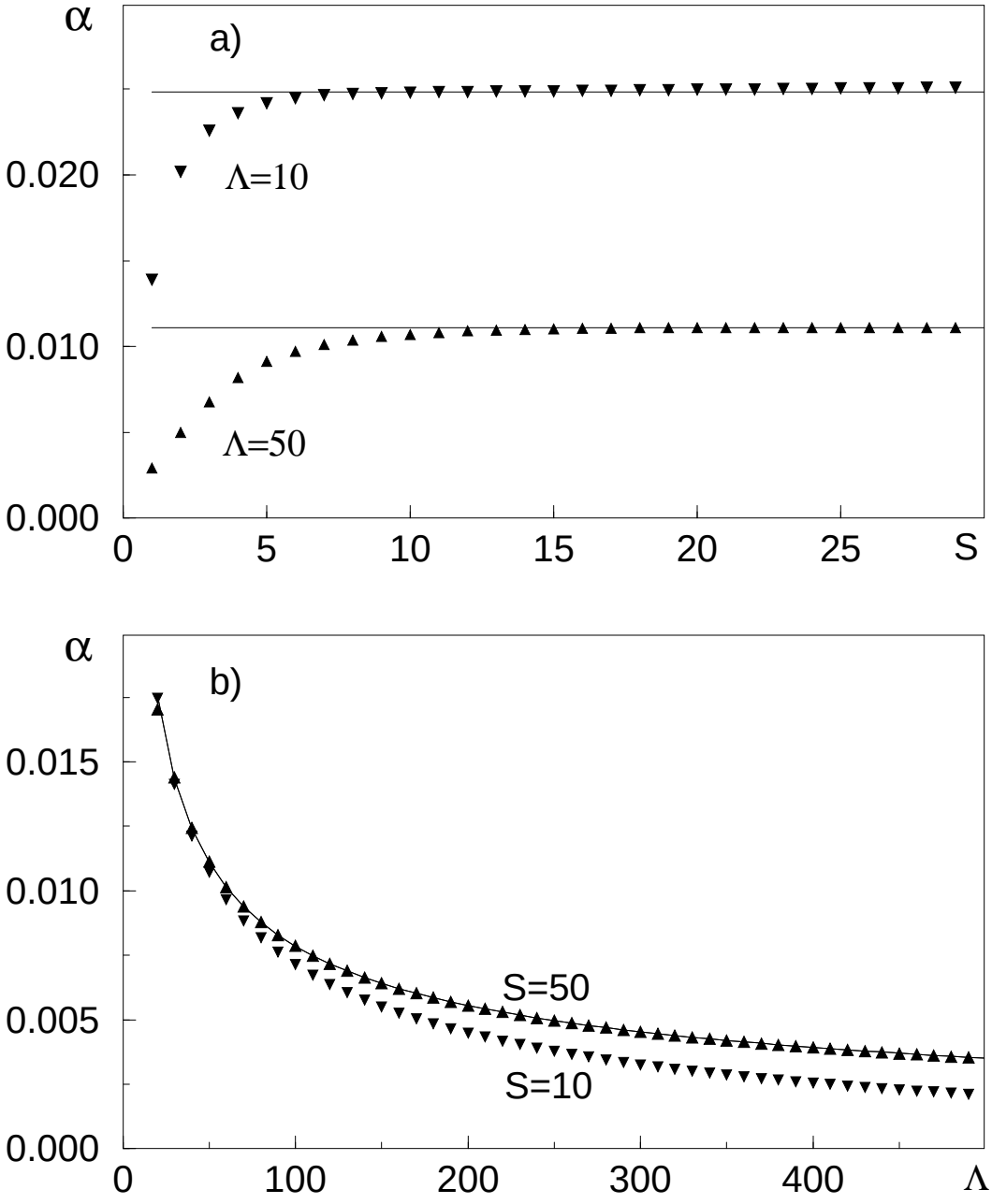
α
a)
0.020
0.010
0.000
Λ=10
Λ=50
0
5
10
15
20
25
S
α
b)
0.015
0.010
0.005
0.000
S=50
S=10
0
100
200
300
400
Λ

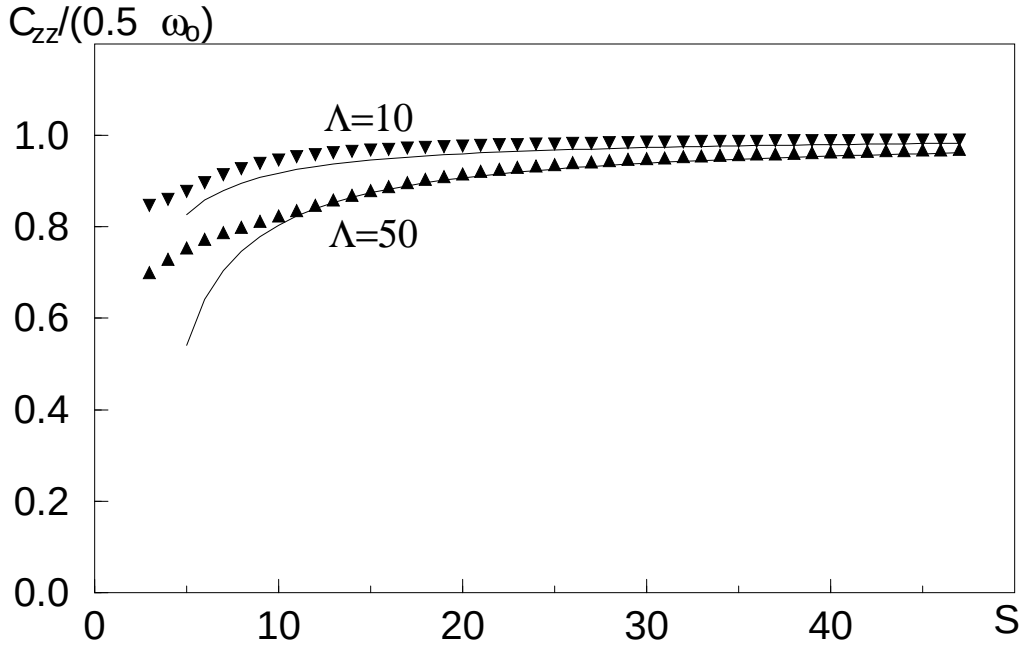
$C_{zz}/(0.5\ \omega_0)$
1.0
0.8
0.6
0.4
0.2
0.0
0
10
20
30
40
S
Λ=10
Λ=50

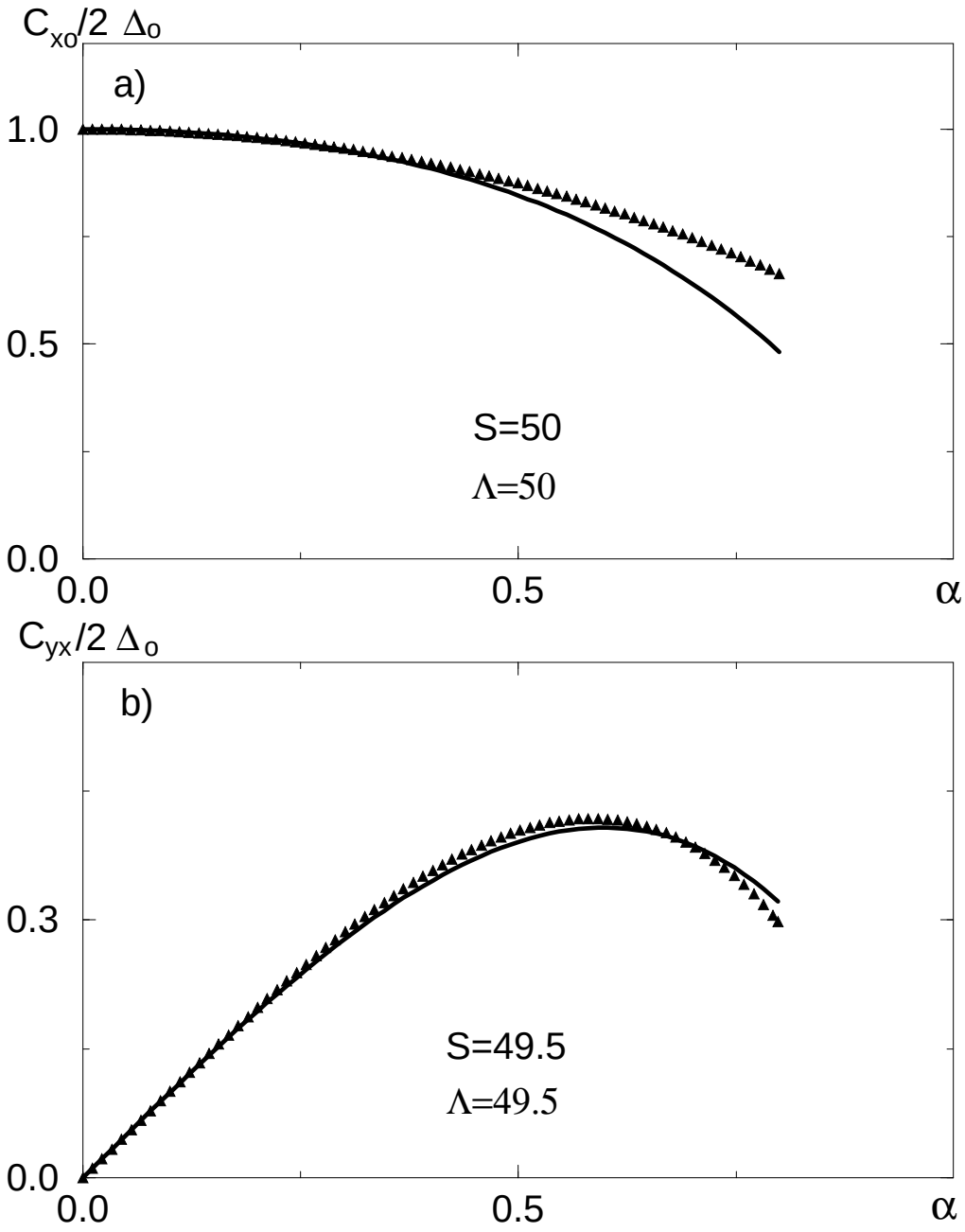
$C_{xo}/2\ \Delta_o$
a)
1.0
0.5
0.0
S=50
Λ=50
0.0
0.5
α
$C_{yx}/2\ \Delta_o$
b)
0.3
0.0
S=49.5
Λ=49.5
0.0
0.5
α